

5-1-2004

# Nonlinear tapping dynamics of multi-walled carbon nanotube tipped atomic force microcantilevers

S. I. Lee

*Purdue University*

S. W. Howell

*Purdue University*

Arvind Raman

*Purdue University, raman@purdue.edu*

R. Reifenberger

*Birck Nanotechnology Center, Purdue University, reifenbr@purdue.edu*

C. V. Nguyen

*ELORET Corporation, NASA Ames Research Center*

*See next page for additional authors*

Follow this and additional works at: <http://docs.lib.purdue.edu/nanodocs>

---

Lee, S. I.; Howell, S. W.; Raman, Arvind ; Reifenberger, R.; Nguyen, C. V.; and Meyyappan, M., "Nonlinear tapping dynamics of multi-walled carbon nanotube tipped atomic force microcantilevers" (2004). *Other Nanotechnology Publications*. Paper 49.  
<http://docs.lib.purdue.edu/nanodocs/49>

This document has been made available through Purdue e-Pubs, a service of the Purdue University Libraries. Please contact [epubs@purdue.edu](mailto:epubs@purdue.edu) for additional information.

---

**Authors**

S. I. Lee, S. W. Howell, Arvind Raman, R. Reifenberger, C. V. Nguyen, and M. Meyyappan

# Nonlinear tapping dynamics of multi-walled carbon nanotube tipped atomic force microcantilevers

S I Lee<sup>1,5</sup>, S W Howell<sup>2,6</sup>, A Raman<sup>1,7</sup>, R Reifenger<sup>2</sup>,  
C V Nguyen<sup>3,4</sup> and M Meyyappan<sup>3</sup>

<sup>1</sup> School of Mechanical Engineering, Purdue University, West Lafayette, IN 47907, USA

<sup>2</sup> Department of Physics, Purdue University, West Lafayette, IN 47907, USA

<sup>3</sup> NASA Ames Research Center, Moffett Field, CA 94035, USA

<sup>4</sup> ELORET Corporation, Moffett Field, CA 94035, USA

E-mail: raman@ecn.purdue.edu

Received 3 October 2003, in final form 15 December 2003

Published 29 January 2004

Online at [stacks.iop.org/Nano/15/416](http://stacks.iop.org/Nano/15/416) (DOI: 10.1088/0957-4484/15/5/002)

## Abstract

The nonlinear dynamics of an atomic force microcantilever (AFM) with an attached multi-walled carbon nanotube (MWCNT) tip is investigated experimentally and theoretically. We present the experimental nonlinear frequency response of a MWCNT tipped microcantilever in the tapping mode. Several unusual features in the response distinguish it from those traditionally observed for conventional tips. The MWCNT tipped AFM probe is apparently immune to conventional imaging instabilities related to the coexistence of attractive and repulsive tapping regimes. A theoretical interaction model for the system using an Euler elastica MWCNT model is developed and found to predict several unusual features of the measured nonlinear response.

(Some figures in this article are in colour only in the electronic version)

## 1. Introduction

Carbon nanotube (CNT) tips attached to scanning probe microcantilevers are considered advantageous in AFM [1] for several reasons: they have small tip radii, a high length-to-diameter aspect ratio, a well-defined atomic configuration, high wear resistance, and significant bending flexibility [2, 3]. Tapping mode imaging using such tips has recently been demonstrated [4]. However, a fundamental understanding of imaging stability and probe vibration response requires an in-depth investigation of the nonlinear dynamics and dynamic buckling of CNT probe tips. Snow *et al* [5, 6] analysed the dynamics of noncontact CNT tips. However, the nonlinear dynamics of tapping with a CNT tip, including the effects

of the buckling of the CNT, has not yet been modelled or measured. Moreover the key differences between the nonlinear response of conventional and CNT tips have not been discussed. To address these issues, experimental and theoretical investigations are undertaken to obtain a description of the highly nonlinear physics of MWCNT AFM cantilevers in the tapping mode.

## 2. Experiments

A CNT AFM tip and a special configuration of an AFM system are utilized to demonstrate the effects of nonlinearities on the tip response. The MWCNT probe (figure 1) is fabricated using a technique [7] that ensures firm binding of the MWCNT to the AFM tip. Note that the MWCNT appears to have extra materials adsorbed onto the surface. This is not uncommon, particularly with amorphous carbon or graphitic nanoparticles, and is unlikely to affect the bulk mechanical properties of the nanotube. A force modulation etched silicon microcantilever (FESP type,  $f_0 = 72.5$  kHz,  $k = 1\text{--}5$  N m<sup>-1</sup>, Digital

<sup>5</sup> Present address: School of Mechanical Design and Automation Engineering, Seoul National University of Technology, 172 Gongneung-dong, Nowon-gu, 139-743, Seoul, Republic of Korea.

<sup>6</sup> Present address: Sandia National Laboratories, Albuquerque, NM 87185, USA.

<sup>7</sup> Author to whom any correspondence should be addressed.

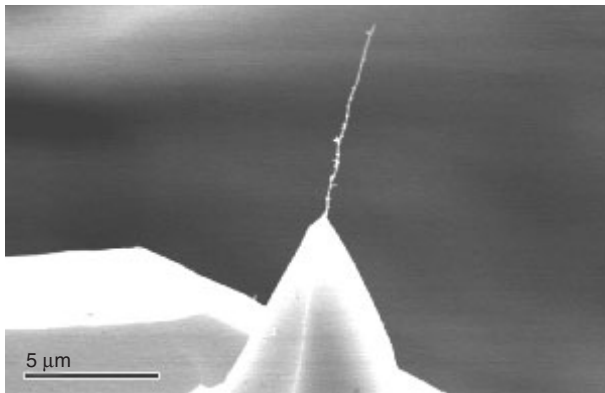


**Figure 1.** The MWCNT probe tip (SEM micrograph) used in the experiments. The MWCNT is approximately  $7.5\ \mu\text{m}$  long and  $10\ \text{nm}$  in diameter.

Instruments Inc.) is employed on a Nanotec<sup>TM</sup> scanning probe microscope. The experimental set-up is described in detail in [8]. Two sets of experiments will be described:

- (a) obtaining a static force–distance curve, and
- (b) obtaining the frequency response of the cantilever amplitude as the excitation is swept through resonance at different tip–sample separations.

The data are reproducible and the CNT tip remained unchanged after the experiments were completed as judged from before and after SEM micrographs.

The complex nature of the tip–sample interaction at various separation distances can cause the MWCNT to buckle as well as slip, slide, and adhere to the surface of the sample depending on the tip–sample separation. These effects can be clearly demonstrated by measuring the static force–distance curve which records the force on the MWCNT tip as a function of the  $Z$  travel distance (figure 2(a)). A schematic diagram of a proposed sequence of CNT deformations consistent with our  $F(Z)$  data is shown in figure 2(b).

As the tip approaches the surface (from A to F), the cantilever first snaps into contact with the sample and then deflects linearly from point B to C as the CNT tip pushes against the surface. From point C the cantilever exhibits a nonlinear deflection with increasing  $Z$ , indicating a buckling of the MWCNT tip. The near constant cantilever deflection beyond point D indicates that the deformation is directed into MWCNT buckling rather than producing additional cantilever deflection. Beyond point E (after  $\sim 800\ \text{nm}$  of indentation), there is a sudden decrease in cantilever deflection, suggesting that the MWCNT has slipped on the HOPG surface.

In contrast, as the tip retracts from the sample ( $F \rightarrow G \rightarrow H \rightarrow A$ ) the high adhesive forces between the bent MWCNT sidewall and the sample ensure that the cantilever deflection remains nearly constant from F until G. From G to H the static force–distance curve is similar to that during approach from B to D, albeit in reverse order. Note however that the curves B to D and G to H do not coincide due to small thermal  $Z$  drifts always present in these experiments. These static force–distance curve measurements have been repeated several times; the results of subsequent experiments are quantitatively and qualitatively very similar barring the slight errors due to thermal drifts.

In a separate set of experiments, we find that the dynamic response of the tapping MWCNT tip is highly nonlinear and displays unusual features that distinguish it from those of conventional scanning probe tips. To demonstrate this, for each tip–sample separation distance, the dither excitation frequency is swept up and down through the microcantilever’s linear resonance frequency. The excitation level of the dither piezoactuator is maintained constant at  $240\ \text{mV}$  for all these experiments. For each frequency increment ( $\Delta f = 25\ \text{Hz}$ ), the amplitude and phase of the cantilever oscillation (referenced to the excitation frequency) are measured by a lock-in amplifier. The tip–sample separation is systematically reduced until the cantilever oscillation displays nonlinear resonance behaviour, indicating physical contact between the CNT tip and the HOPG surface. Figure 3(a) shows representative results of the near resonant response near resonance in air when (i) the tip is far away from the sample, (ii) the tip–sample separation is  $\sim 65\ \text{nm}$ , and (iii) the tip–sample separation is  $\sim 45\ \text{nm}$ .

When the CNT tip is far away from the sample, the response is essentially linear. As the tip–sample separation is reduced to  $\sim 65\ \text{nm}$ , the amplitude of oscillation is reduced, and saturates in the frequency range where the CNT tip taps gently on the sample. At  $\sim 45\ \text{nm}$  tip–sample separation, the amplitude response is further reduced and develops a distinct feature on the otherwise saturated amplitude region of the tapping mode response. The amplitude and phase response at the tip–sample separation of  $\sim 45\ \text{nm}$  are shown in more detail in figure 3(b). Two jumps are clearly observed in the phase response (at  $72.4$  and  $72.6\ \text{kHz}$ ). The unexpected *increase* of the tip amplitude in the saturated tapping response region suggests a dynamic buckling of the MWCNT. As the tip–sample separation is decreased further, the cantilever’s amplitude of oscillation increases somewhat, a result that is consistent with the buckling of the MWCNT tip.

Several important features of this nonlinear response are considerably different from those observed for similar stiffness Si tips tapping on similar HOPG samples [8, 9]. First, the CNT tip does not exhibit multiple oscillation states. This is very different from the case for conventional tips where over a wide range of frequencies, a repulsive and attractive mode of imaging coexist. Secondly, in conventional tips, phase jumps usually occur at the extremal frequencies where the cantilever amplitude becomes saturated. However in the present case, no phase jump accompanies the higher frequency at which amplitude saturation is achieved during tapping. The apparent non-coexistence of attractive and repulsive imaging modes implies higher stability and could offer significant advantages over conventional tips [10–12]. Note that [13] have shown that the non-coexistence of attractive and repulsive regime oscillations can also be achieved with conventional silicon tips using subtle control of appropriate experimental parameters. With the present CNT tip, however, the non-coexistence of attractive and repulsive regimes was observed over a wide range of tip–sample gaps, and this behaviour appears to be the norm rather than an exception. The above reproducible results were presented for a specific CNT probe, and clearly more experimental results with a variety of different CNT probes are needed to generalize these results.

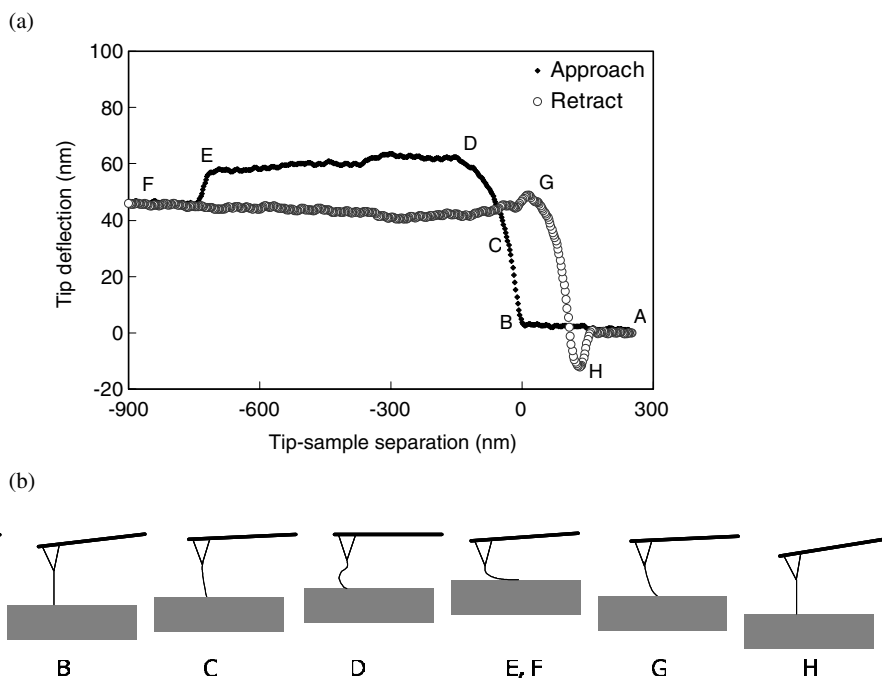


**Figure 2.** (a) The static force–distance curve of the CNT tip on HOPG surface. The tip–sample approach process starts at the tip–sample separation  $Z = 250$  nm. Also this  $F(Z)$  curve shows  $\sim 80$  nm of thermal  $Z$  drift between approach and retraction processes. (b) A schematic diagram of the tip deflection during approach and retraction.

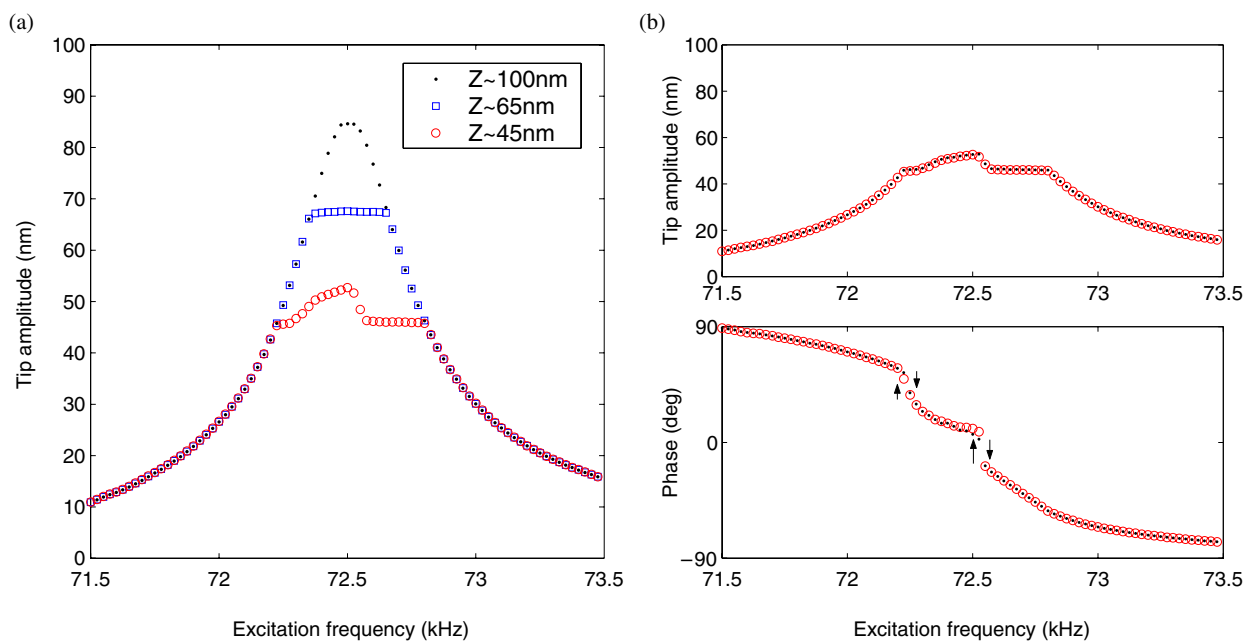


**Figure 3.** The cantilever tip amplitude and phase (w.r.t. driving frequency) of the carbon nanotube tip over HOPG surface. In (a), a plot of the amplitude response for different  $Z$ . In (b), the amplitude and phase response at  $Z = 45$  nm. The circles indicate the response during frequency sweeping up; the dots represent the response during frequency sweeping down.

### 3. Theoretical analysis

To predict the nonlinear response of the CNT tipped microcantilever, the MWCNT is modelled using the Euler elastica [14, 15]<sup>8</sup>. In what follows, we focus on the prediction

<sup>8</sup> The use of a rod-like continuum model of the MWCNT is justified because of the very large length-to-diameter ratio ( $\sim 750$ ) of this probe tip [16].

of microcantilever vibration, and not on the MWCNT vibration. Accordingly the primary goal of the MWCNT model is to correctly predict the normal force transferred via the MWCNT from the sample to the microcantilever. Several simplifying assumptions are made towards this goal.

First, the mass of the CNT is infinitesimal compared to that of the microcantilever. Accordingly, the MWCNT lateral

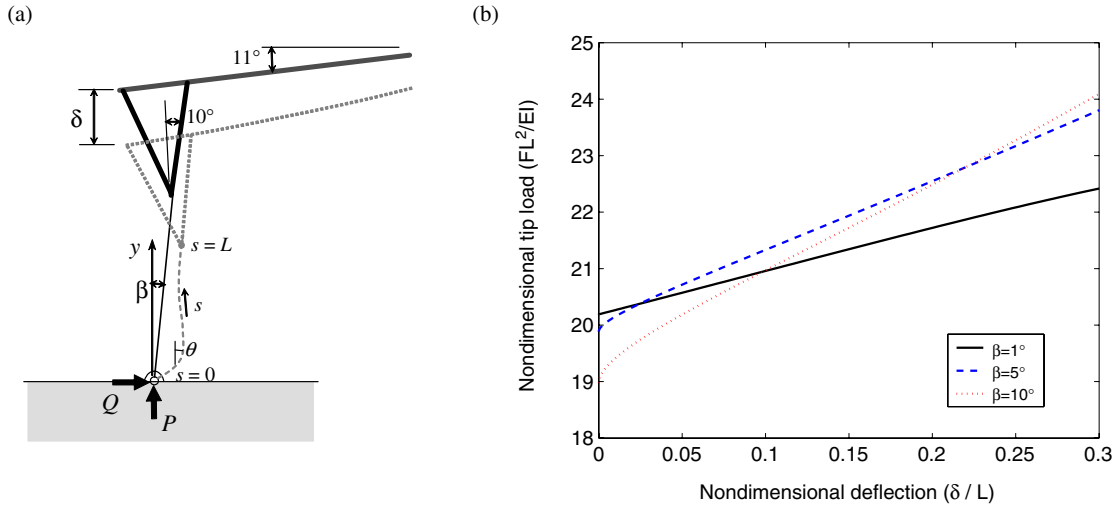


**Figure 4.** (a) The theoretical model (Euler elastica) of the MWCNT probe with the clamped–pinned boundary condition, and (b) the tip load–deflection curve from the theoretical model. In (a),  $L$  is the length of CNT probe,  $\delta$  is the deflection of the tip,  $s$  is the coordinate along the CNT probe, and  $\theta$  is the deflection angle of the CNT probe.  $P$  and  $Q$  are respectively the normal and lateral reactions at the pinned end. In (b),  $F$  is the resultant load exerted on the microcantilever obtained by  $P \cos \beta + Q \sin \beta$ , and  $E$  and  $I$  are the elastic modulus and the area moment of inertia of the CNT.

inertia contribution to the interaction force is neglected and it is assumed that the MWCNT deforms quasi-statically during tip–sample impact. Secondly, it is assumed that the MWCNT is oriented identically with respect to the sample before each impact<sup>9</sup>. Figure 4(a) illustrates this idea and shows the nominal experimental values of microcantilever slant angle and the half-cone angle of the pyramidal silicon tip to which the MWCNT is attached. The nominal contact angle  $\beta$  is  $1^\circ$ . Furthering the experimental static force–distance curve for this tip (figure 2) indicates that MWCNT sliding occurs at very large ( $\sim 800$  nm) indentation depths. It is reasonable therefore to assume that in the regime of light tapping, the MWCNT does not slip on the surface. Therefore to model the tapping response, we assume that the CNT probe is clamped at the tip and pinned without sliding on the sample surface when it is in contact with the surface.

The equation for the elastica deformation in terms of the variables described in figure 4(a) is

$$EI \frac{d^2 \theta}{ds^2} + P \sin \theta + Q \sin \theta = 0, \quad \text{with } 0 \leq s \leq L, \quad (1)$$

and the end conditions and geometric constraints are

$$\left. \frac{d\theta}{ds} \right|_{s=0} = 0, \quad \theta|_{s=L} = \beta, \quad \frac{dy}{ds} = \cos \theta,$$

$$y|_{s=0} = 0, \quad \text{and} \quad \int_0^L \sin \theta \, ds = L \sin \beta.$$

The cantilever tip deflection is obtained as

$$\delta = L \cos \beta - \int_0^L \cos \theta \, ds.$$

<sup>9</sup> It is reasonable to assume that the first bending frequency of the MWCNT used here is 300 kHz with a  $Q$  factor of 500 [17]. It follows that the transient MWCNT vibrations do not damp out completely before a subsequent impact. However in the experiments, the MWCNT buckles only slightly so that the transient MWCNT flexural vibrations, and consequently the variations in the MWCNT orientation preceding each impact, are assumed to be negligible.

Equation (1) can be solved numerically for several values of the contact angle  $\beta$  using a numerical continuation technique AUTO which is a powerful computational tool for investigating nonlinear solutions of differential equations [18]. The normalized load–deflection curves we calculate are plotted in figure 4(b). Note that these force–deflection curves bear no resemblance to that expected for a harmonic system since deflection is not proportional to normalized force. Instead, for a range of applied forces up to a threshold value, the system exhibits *no* deflection until a threshold force is reached. Beyond this threshold, the CNT begins to flex. Further, from the calculations, small variations ( $1^\circ$ – $5^\circ$ ) in the contact angle  $\beta$  do not cause a large variation in the buckling force. This result is important because it predicts relatively minor effects for small variations in CNT orientation between successive impacts.

The CNT force–deflection curve for a nominal  $\beta = 1^\circ$  has been used to construct a tip–sample interaction model for the dynamic tapping mode microcantilever response. Let the interaction force be specified by a piecewise continuous  $F_i(z)$  where  $z$  is the instantaneous CNT–sample separation. For the system studied here, when  $z > a_0$  ( $a_0$  denotes the intermolecular distance when the CNT tip contacts the HOPG surface),  $F_i(z)$  consists of carbon–carbon van der Waals force between a nominal 10 nm diameter sphere and an infinite half-space. When  $z \leq 0$ ,  $F_i(z)$  is derived from the linear approximation of the CNT force–deflection curve immediately following the threshold buckling load (see figure 4(b)). When  $0 < z \leq a_0$ ,  $F_i(z)$  is approximated as a quadratic polynomial such that  $F_i(z)$  is smooth at  $z = 0$  and simultaneously continuous at  $z = a_0$ . The use of a quadratic polynomial in the small  $z$  range circumvents the mathematical complications associated with discontinuous force interactions. This model is also more realistic because the CNT is always slightly curved resulting in an imperfect bifurcation which leads to a smooth buckling curve.

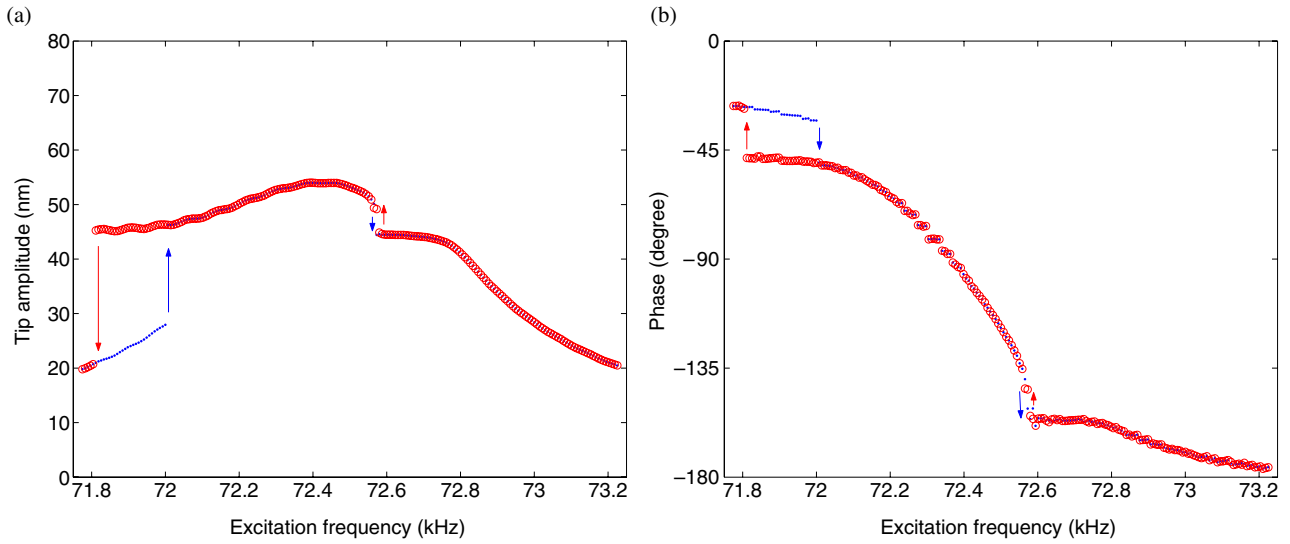


**Figure 5.** MATLAB simulation results for frequency response: rms amplitude (a) and phase (b). Dots: frequency sweeping up; and circles: frequency sweeping down.

Accordingly, the interaction force can be written as

$$F_i(z) = \begin{cases} \frac{C_1}{z^2} & (\text{for } z > a_0), \\ C_2 - C_3z + \frac{1}{a_0^2} \left( \frac{C_1}{a_0^2} - C_2 + C_3a_0 \right) z^2 & (\text{for } 0 < z \leq a_0), \\ C_2 - C_3z & (\text{for } z \leq 0), \end{cases} \quad (2)$$

where  $C_1$ ,  $C_2$ , and  $C_3$  are constants. A modal contact damping [9] is also introduced for simulating the additional dissipation encountered when the CNT contacts the sample. This interaction model is then applied to the dynamic equation for the driven microcantilever developed in [8]. Geometric and material properties of the experimental microcantilever needed for relevant parameters in the dynamic equation are derived from manufacturer specified data and textbook values<sup>10</sup>. The bending stiffness  $EI$  of MWCNT and the modal contact damping factor are fitted to match features of the experimental nonlinear response data<sup>11</sup>.

MATLAB simulations were performed to obtain the dynamic response of the theoretical model for  $Z \sim 45$  nm. Figure 5 describes the frequency response of the amplitude and phase. Apart from reproducing the overall shape of the resonance curve when the CNT tip is buckling, the theoretical predictions clearly capture two essential features in the measured response:

<sup>10</sup> Cantilever length = 225  $\mu\text{m}$ ; cantilever width = 15  $\mu\text{m}$ ; cantilever thickness = 2.6  $\mu\text{m}$ ; tip radius = 5 nm; fundamental resonance frequency = 72.5 kHz; spring constant of the cantilever = 1 N m<sup>-1</sup>;  $Q$  factor = 180; Hamaker constant (C-C) =  $3.19 \times 10^{-19}$  J; base driving amplitude = 0.27 nm.

<sup>11</sup> We assume five shells comprise the MWCNT; CNT probe length = 7.5  $\mu\text{m}$ ; CNT diameter = 10 nm; the CNT's  $EI$ ,  $\sim 2 \times 10^{-22}$  N m<sup>2</sup>, is fitted by matching the theoretical prediction with the experimental excitation frequency at which the CNT first buckles while the frequency is swept down across the resonance; the CNT's mass density is  $\sim 1890$  kg m<sup>-3</sup>; the modal contact damping factor ( $Q$  factor = 18) is fitted to match the experimental amplitude of the maximum microcantilever amplitude achieved in the frequency range where the CNT buckles dynamically.

- (i) the unexpected increase of the amplitude in the saturated tapping response region, and
- (ii) the two distinct phase jumps which closely correspond to the frequencies measured from experiment.

There are some notable differences from the experimental data at the lower frequencies along the saturated amplitude branch. It is likely that these discrepancies are caused because

- (a) the spherical tip approximation overpredicts van der Waals forces on a CNT [5] especially when the MWCNT end is oxidatively opened and contains oxygen functional groups, and
- (b) the vibrations of the CNT may not be negligible in that frequency range.

In addition to calculations predicting the CNT tip behaviour as a function of driving frequency, the fundamental frequency of oscillation was computed using MATLAB simulations for the undamped, unforced cantilever system as a function of initial tip displacement from equilibrium. A plot of tip amplitude versus resonant frequency is referred to as a backbone curve [19] and is a very useful tool for analysing the nonlinear effects in the forced, damped system. The results for a tip-sample separation of 45 nm are plotted in figure 6. The initial decrease in resonant frequency (softening [19]) as the tip amplitude is increased is due to the van der Waals attractive interactions. The subsequent increase in resonant frequency (hardening [19]) is from the buckling nonlinearity of the CNT probe.

The primary differences between the backbone curve for conventional tips [8] and the present case are that

- (i) the MWCNT probe tip exhibits a very gentle hardening nonlinearity, and
- (ii) the nonlinear response is dominated by attractive interactions except in the small frequency range where the CNT buckles.

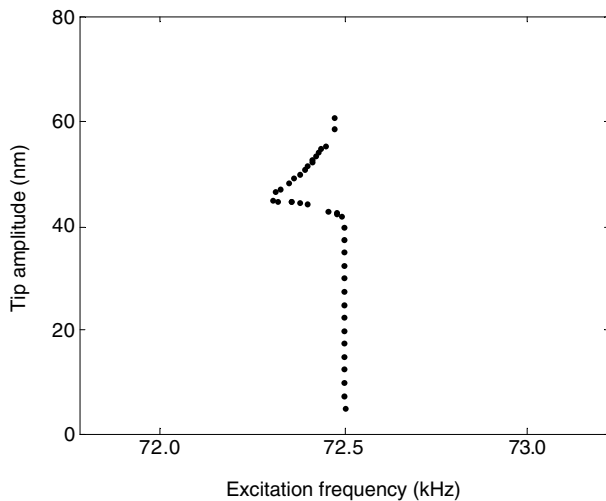


**Figure 6.** The MATLAB simulation result: the backbone curve for the amplitude response for a tip-sample separation of 45 nm.

#### 4. Conclusion

In conclusion, the nonlinear frequency response of a  $7.5 \mu\text{m}$  long MWCNT attached to an AFM microcantilever tapping on a graphite sample has been investigated both theoretically and experimentally. We find a nonlinear behaviour that is considerably different from those of conventional tips. The Euler elastica model for the MWCNT provides a good first approximation for the tip-sample interaction potential which leads to reasonably predictive models for the tapping mode response.

#### Acknowledgments

The corresponding author (AR) gratefully acknowledges financial support for this research from the National Science

Foundation under award No 0116414-CMS, and by NASA under award No NCC 2-1363. One of the authors (CVN) is supported through a contract from NASA to ELORET Corp.

#### References

- [1] Dai H, Hafner J H, Rinzler A G, Colbert D T and Smalley R E 1996 *Nature* **384** 147–50
- [2] Li J, Cassell A M and Dai H 1999 *Surf. Interface Anal.* **28** 8–11
- [3] Stevens R M D, Frederick N A, Smith B L, Morse D E, Stucky G D and Hansma P K 2000 *Nanotechnology* **11** 1–5
- [4] Moloni K, Buss M R and Andres R P 1999 *Ultramicroscopy* **80** 237–46
- [5] Snow E S, Campbell P M and Novak J P 2002 *Appl. Phys. Lett.* **80** 2002–4
- [6] Snow E S, Campbell P M and Novak J P 2002 *J. Vac. Sci. Technol. B* **20** 822–7
- [7] Nguyen C V, Chao K-J, Stevens R M D, Delzeit L, Cassell A, Han J and Meyyappan M 2001 *Nanotechnology* **12** 363–7
- [8] Lee S I, Howell S W, Raman A and Reifenberger R 2002 *Phys. Rev. B* **66** 115409
- [9] Lee S I, Howell S W, Raman A and Reifenberger R 2003 *Ultramicroscopy* **97** 185–98
- [10] Kühle A, Sørensen A H and Bohr J 1997 *J. Appl. Phys.* **81** 6562
- [11] García R and San Paulo A 1999 *Phys. Rev. B* **60** 4961
- [12] García R and San Paulo A 2000 *Phys. Rev. B* **61** R13381
- [13] San Paulo A and García R 2002 *Phys. Rev. B* **66** R41406
- [14] Love A E H 1944 *A Treatise on the Mathematical Theory of Elasticity* (New York: Dover)
- [15] Wang C Y 1997 *Int. J. Non-Linear Mech.* **32** 1115–22
- [16] Harik V M 2002 *Comput. Mater. Sci.* **24** 328–42
- [17] Poncharal P, Wang Z L, Ugarte D and de Heer W A 1999 *Science* **283** 1513–6
- [18] Doedel E J, Champneys A R, Fairgrieve T F, Kuznetsov Y A, Sandstede B and Wang X 1997 *AUTO 97: Continuation and Bifurcation Software for Ordinary Differential Equations* Concordia University
- [19] Nayfeh A H and Mook D T 1995 *Nonlinear Oscillations* Wiley Classics Library Edition (New York: Wiley)